ARTICLE TYPE www. rsc.org/xxxxxx | XXXXXXXX

Fingerprinting Seamless Single-Walled Carbon Nanotube Junctions via Migration of Encapsulated N_2 Molecules

From bottom to top, are arrays of vertically aligned SWNT continuous?

Theerapol Thurakitseree,*[a] Christian Kramberger,[b] Pisith Singjai,[c] and Shigeo Maruyama*[d,e]

Received Xth XXXXXXXXXX 20XX, Accepted Xth XXXXXXXXX 20XX
First published on the web Xth XXXXXXXXXX 200X
DOI: 10.1039/b000000x

Structure control such as diameter changes along single-walled carbon nanotubes (SWNTs) can be achieved in arrays of vertically aligned (VA-) SWNTs by switching the feedstock during growth. The local nature of the macroscopic transition from one diameter to another is then questioned as one can either envisage seamless transitions or discontinuous individual SWNTs. Here, we demonstrate that encapsulated molecules can serve as markers to doubtlessly identify seamless interconnections in macroscopic samples. A migration of nitrogen molecules inside continuous SWNTs is observed by bulk scale measurements on double-layered SWNT array synthesized from different carbon/nitrogen feedstocks. The existence of N_2 molecules at the top of the SWNT array proves continuous SWNTs throughout double layered arrays with different diameters.

1 Introduction

Structure control of single-walled carbon nanotubes (SWNTs) during the growth process is a long standing goal. It can be achieved by altering the nanotube diameter as it dictates the possible chiralities. Changing diameters can be triggered by controlled changes in synthesis conditions [1–5]. The nanotube diameter could be changed along the tube during the reaction by changes in growth temperature [3–5], so that a distinct structures could be obtained on the same nanotube due to lattice distortions [6]. S. K. Doorn *et al.* [3] have reported coincidental changes in nanotube diameter of ultralong SWNTs along the tube during the growth process by tracing with confocal Raman imaging. These changes on individual SWNTs were explained with pairs of pentagon-heptagon defects. The thermal effect on molecular junction has also been demonstrated in multi-walled carbon nanotubes [2]. A well-controlled growth of intramolecular junction was performed by temperature modulated growth [4]. Y. Yao *et al.* [4] have reported that SWNT diameter can change with the formation of intramolecular junction between SWNT sections grown with different temperatures. Even though SWNTs with intramolecular junction could be grown by several methods [1–5], the observations were performed on individual nanotubes. Bulk confirmation of intramolecular junctions throughout macroscopic samples are still elusive.

In our previous report [7], we have addressed the interconnection between nanotubes in multi-layered VA-SWNT arrays by tracing the apparent morphology of SWNT along the vertical direction that exhibits different mean diameters. After mechanical cleavage, naturally resulting in discontinuities, TEM data still confirmed individual intact intramolecular junctions. This naturally posses the question for possibly more abundant intramolecular junctions in pristine as grown material. Since acetonitrile is used as a carbon/nitrogen (C/N) feedstock to reduce nanotube diameter [7], a by-product that comes along with the reaction are N_2 molecules which are encapsulated inside the nanotube host. With the encapsulated N_2 molecules in mind the question for continuous SWNT in a diameter modulated multilayer array is equivalent to 1D diffusion of those molecules from one layer to another.

Here, we demonstrate seamless SWNT connection on the *bulk* scale by tracing the existence of N_2 molecules inside continuous SWNT in double-layered SWNT arrays. An acetonitrile/ethanol mixture was used as C/N feedstock and N_2 source. By spectroscopic analysis, a migration of encapsu-

[a] *Maejo University, Chiang Mai, Thailand. Fax: 66 53 878225; Tel: 66 53 873515; E-mail: theerapol@mju.ac.th*
[b] *University of Vienna, Vienna, Austria.*
[c] *Chiang Mai University, Chiang Mai, Thailand.*
[d] *University of Tokyo, Tokyo, Japan. Fax: 81 3 5800 6983; Tel: 81 3 5841 6421; E-mail: maruyama@photon.t.u-tokyo.ac.jp*
[e] *National Institute of Advanced Industrial Science and Technology, Tsukuba, Japan.*

lated N_2 was found to occur from the bottom layer where SWNTs contain gas molecules to the top layer of empty nanotubes. The observed N_2 content at the top layer demonstrates ubiquitous seamless nanotubes junctions.

2 Materials & Methods

The double-layered VA-SWNT arrays were grown on silicon substrates by no-flow CVD.[8] Cobalt (Co) and molybdenum (Mo) acetate prepared by a dip coating process were used as a binary catalyst with the concentration of 0.1 wt.% each.[9] The Co/Mo catalyst was initially reduced under Ar containing 3% H_2 atmosphere. After the temperature has reached 800°C, 40 μL of pure ethanol (EtOH) were firstly introduced into the CVD chamber, and the first stage of the CVD reaction was kept for 90 s at a pressure of about 1.4 to 2.3 kPa. Prior to introduction of 10% mixed acetonitrile ethanol feedstock (10% AcN), the CVD chamber was evacuated to the background pressure of 14 Pa with the dwell time of 30 s. 40 μL of 10% AcN feedstock were then released into the chamber. N-doped SWNT arrays were continuously grown for another 150 s. The CVD chamber was finally cooled down to room temperature. Double layered samples obtained by this procedure are hereafter referred to as $SWNT_{Et\text{-}Ac}$. Samples consisting of only one single layer grown from one feedstock are labelled $SWNT_{Et}$ and $SWNT_{Ac}$, respectively.

The morphology of VA-SWNT arrays was investigated by scanning electron microscopy (SEM, 1 kV acceleration voltage, S-4800, Hitachi Co., Ltd.). As-grown VA-SWNT arrays were characterized by resonance Raman spectroscopy (Chromex 501is with Andor DV401-FI) using an excitation wavelength of 488 nm and spectrometer grating of 1800 lines/mm with the laser spot size of about 2 μm in diameter[10]. The incident laser with a power of 0.25 mW was focused by a 50× objective lens. For cross sectional Raman measurements the polarization was kept perpendicular to the nanotube axis to minimize laser heating effect[11]. For photoelectron spectroscopy (XPS), VA-SWNT arrays were firstly heated at 400°C in vacuum (14 Pa) to desorb H_2O and N_2 molecules before the measurement. The XPS spectra were measured with a PHI 5000 VersaProbe setup with 1.486 keV and the beam size of 100 μm in diameter. The pass energy of 23.5 eV with the energy step of 0.1 eV were set for the measurement of C1s and N1s core levels. For control experiments, $SWNT_{Ac}$ and $SWNT_{Et}$ were annealed in air at 500°C for 10 min to remove the nanotube cap[12] and release the encapsulated N_2 molecules.

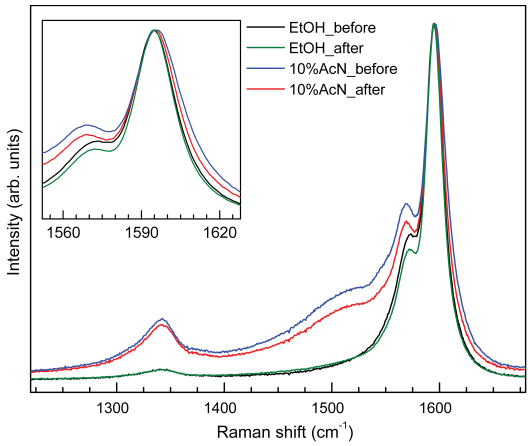

Fig. 1 A comparison of resonance Raman spectra of SWNTs synthesized from ethanol (EtOH) and 10% acetonitrile (10% AcN) before and after annealing at 500°C for 10 min.

3 Results & Discussion

3.1 Signatures of encapsulated N_2

Fig. 1 shows the comparison of G-band linewidth before and after cap-opening annealing of $SWNT_{Et}$ and $SWNT_{Ac}$. The G-Band is observed at 1594 cm^{-1}. The prominent Breit-Wigner-Fano (BWF) lineshape and higher D-band intensity is at this wavelength a distinct feature of $SWNT_{Ac}$, thus they can be distinguished from $SWNT_{Et}$. The G-bands were fitted using one fixed Fano lineshape at 1571 cm^{-1}, one fixed Lorentzian peak at 1607 cm^{-1}, and one free Lorentzian peak for EtOH case, as well as, one fixed Fano lineshape at 1521 cm^{-1}, five fixed Lorentzian peaks at 1486, 1552, 1568, 1607 cm^{-1}, and one free Lorentzian peak for 10% AcN case (see in Fig. S1). The G-band linewidth of $SWNT_{Ac}$ sharpens after annealing in air, while its frequency is unchanged, its full width at half maximum (FWHM) is narrower by approximately 1.1 cm^{-1}. This constriction of the G-band linewidth indicates the disappearance of the harmonic coupling of trapped N_2 molecules and carbon atoms in the nanotubes. Consistently, there is no such change in the G-band linewidth for $SWNT_{Et}$.

Shortening of the phonon life-times[13] indicates the interaction between encapsulated N_2 molecules specifically inside not-annealed 10% AcN-grown SWNTs with the nanotube host as seen in narrower G-band linewidth (Fig. 1). The carbon structures forming a nanotube cap are readily removed by annealing at 500°C, due to their increased reactivity[12,14]. The control experiment also demonstrates that encapsulated N_2 are mobile and can reach the open end due to weak bonding with graphitic carbon walls as observed in multi-walled carbon nanotubes[15].

The presence of N_2 molecules was also directly detected by XPS measurements. Fig. 2 shows a comparison of XPS spectra of $SWNT_{Ac}$ before and after annealing. The well-defined asymmetric Doniach Šunjić lineshape of the C1s peaks at 284.6 eV with $\pi - \pi^*$ electron shake up is a common feature of SWNTs.[16,17] The binding energy at about 404 eV identifies N_2 molecules inside N-doped SWNT hosts[18]. The N content was evaluated using relative XPS peak areas with the relative atomic cross section of 1.8 for N/C[19]. The abundance of N_2 molecules was found to be approximately 0.3 at.% in pristine $SWNT_{Ac}$, while the signal of N after annealing is well within the noise level. The disappearance of the N_2 signal at the binding energy of 404 eV after opening the cap by annealing is consistent with the Raman data and confirms the escape of N_2 from the interior of SWNTs. The easy removal of linear arrangements of N_2 inside SWNTs is strongly contrasted by gas molecules trapped inside more complex crystal structures, where the escape path is sterically blocked[20]. Note that the observed binding energy of encapsulated N_2 molecules is lower than that of free molecular gaseous N_2 (409.9 eV)[21]. This can be explained by electron screening for N1s core-holes due to surrounding cylinder of sp^2 carbon.[22]

Additionally, a shift in the C1s peak of approximately 0.1 eV without broadening (Fig. 2) was observed. While the hosting SWNT walls can provide the dielectric environment for screening the N1s core level in the encapsulated N_2, the reversed mechanism for N cannot occur. 0.3 at.% of N cannot affect the macroscopic average screening of the C1s core-hole excitation. We argue that this shift is rather due to the different C1s binding energies in metallic and semiconducting SWNTs[23], and the fact that small diameter metallic SWNTs are also more susceptible to oxidation. This interpretation is also in line with the reduced strength of the Fano component in the G-line in annealed SWNTs (Fig. 1).

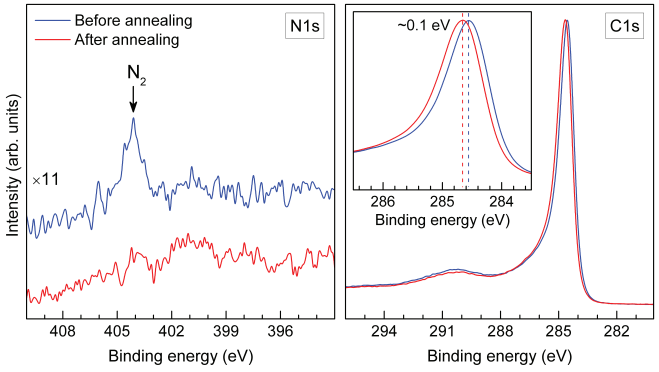

Fig. 2 Photoemission spectra of N-doped SWNT films synthesized from 10% acetonitrile feedstock mixture in ethanol before and after annealing in air at 500°C. The disappearance of N_2 signal was observed after annealing.

3.2 Migration of N_2 molecules

Two differently stacked SWNT arrays from EtOH and 10% AcN grown SWNTs were synthesized by introducing the two carbon feedstocks in sequence. Fig. 3 shows the interface between the layers obtained at the successive stages of the growth, and shows interconnectivity at the length scale of SWNT bundles. The interface is highlighted by yellow arrows. Starting with EtOH feedstock, the initial growth of SWNTs was observed with a thickness of about 5 μm, whereas 6.5 μm of the bottom layer are grown from 10% AcN. The visible interface between the layers are interpreted as recorded changes in growth rates and feedstock flux. Note that the actual growth was halted for 30 s during the feedstock change. Similar horizontal bands were observed in incremental growth with pulsed carbon flux[24].

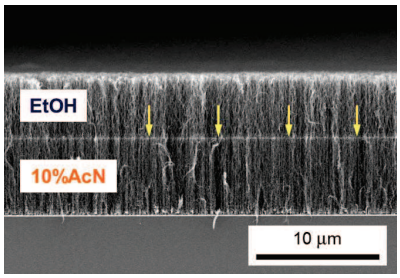

Fig. 3 SEM micrographs of double-layered N-doped SWNT array synthesized from ethanol (EtOH) and 10% acetonitrile feedstock mixture in ethanol (10% AcN), respectively. Yellow arrows highlight the interface between different SWNT arrays at which the feedstock was switched.

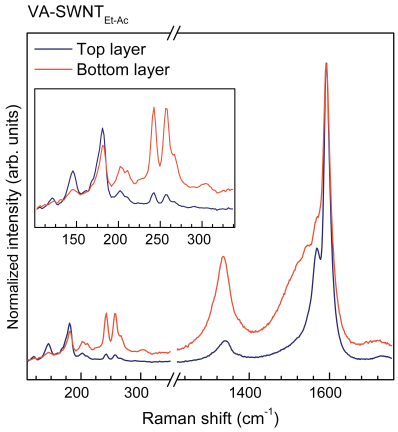

Fig. 4 Cross-sectional resonance Raman spectra of a double-layer VA-SWNT array synthesized from ethanol (top) and 10% acetonitrile (bottom), respectively, indicating root growth mechanism according to feedstock sequence with different nanotube diameters.

The cross sectional Raman spectra of layered samples clearly demonstrate spectral features of $SWNT_{Ac}$ and $SWNT_{Et}$ [7] in the corresponding layers (Fig. 4). The feedstock sequence and layer sequence do match the root growth mechanism[8]. As shown in our earlier report [7], the small-diameter RBM peaks in the range of 100-400 cm^{-1} are predominant for N-doped SWNTs. Fig. 5 shows the comparison of resonance Raman spectra of SWNT arrays synthesized from pure EtOH and $SWNT_{Et\text{-}Ac}$ array. The top surface of the films was measured in both cases.

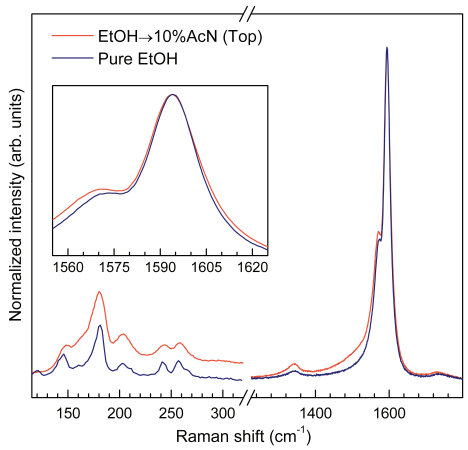

Fig. 5 Raman spectra of a single layered array of $SWNT_{Et}$ from pure EtOH and a layer of $SWNT_{Et}$ with a subsequent layer of $SWNT_{Et\text{-}Ac}$ underneath. The excitation wavelength was 488 nm.

The RBM peaks at 145 and 180 cm^{-1} at 488 nm excitation are a well known feature for vertical aligned arrays[25]. The broadening of the G-band linewidth in $SWNT_{Et\text{-}Ac}$ array can be seen in the inset in Fig. 5. It suggests that there are, like in the case of $SWNT_{Ac}$, N_2 molecules trapped inside the top layer of $SWNT_{Et\text{-}Ac}$.[13]

XPS measurements were performed on the top surface of $SWNT_{Et\text{-}Ac}$ as shown in Fig. 6, to demonstrate the presence of diatomic N_2 molecules in the top layer of double-layered SWNT array where the nanotubes were initially grown from EtOH. The survey scan in the inset shows the strong C1s core level of carbon with absent O_2 absorption after sample annealing.

The signatures of trapped N_2 molecules inside EtOH-grown SWNTs (top layer) is confirmed by the notable peak at the binding energy of 404 eV. This proves the migration of N_2 molecules from the bottom (10% AcN) layer to the top (EtOH) layer. Note that a 5 μm thickness of the top layer is far beyond the escape depth of photoelectrons in homogeneous SWNT arrays. The signal from diatomic N_2 is therefore not attributed to the interface region where the feedstock was switched from EtOH to 10% AcN, or even the bottom layer.

The N content in form of N_2 molecules in the top layer is found to be approximately 0.07 at.% (compare to 0.3 at.% in $SWNT_{Ac}$). This data represents a bulk signature of continuous SWNT throughout a macroscopic sample. In a first approximation disregarding different diameters as well as differences in the thickness of the layers, one would expect to observe about half of the atomic N concentration in double layered $SWNT_{Et\text{-}Ac}$, if all SWNT were running continuously from the bottom of the bottom layer all the way to the top of the top layer. By reversing this estimate we conclude that the fractions of discontinued and continuous SWNT throughout the layers and across the interface are of the same magnitude. The high temperature, uniform electrostatic interaction and pronounced 1D collective diffusion[26] facilitate the equilibration of N_2 among interconnected $SWNT_{Ac}$ and $SWNT_{Et}$ during synthesis. Considering that the growth is halted for 30 s during the exchange of feedstocks which should be expected to favor discontinued SWNTs, we have demonstrated that SWNTs in VA-SWNTs diameter controlled CVD growth can yield bulk material of continuous SWNT featuring intramolecular junctions.

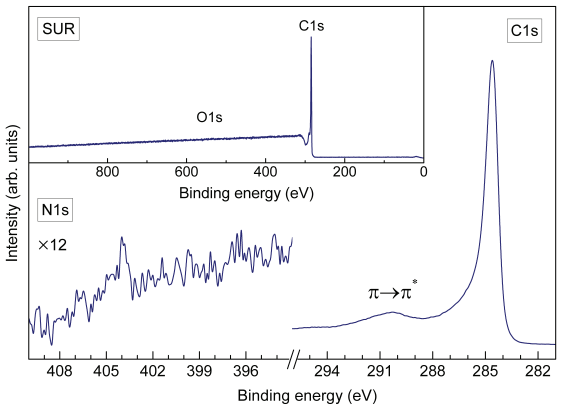

Fig. 6 XPS spectra performed on the top of vertically aligned double-layered SWNT array synthesized from EtOH and 10% AcN, respectively. The molecular N_2 N1s core level is visible. The inset shows the survey scan, indicating very clean sample.

4 Conclusions

The Raman and XPS signatures of encapsulated nitrogen molecules inside N-doped SWNTs were presented. The nanotube cap could be opened by annealing in air to release the trapped molecules. The presence of and disappearance of N_2 were detected by photoemission. The Raman spectra reveal a characteristic broadening and sharpening of the G-band, with the presence and removal of N_2. The XPS data shows in the lowered N1s binding energy the effect of the surrounding matrix on the encapsulated N_2, while Raman spectroscopy probes the effect of the encapsulated N_2 on the hosting SWNT. Both

effects change consistently upon release of the N_2 and conclusively evidence the migration of N_2 molecules inside continuous SWNTs in double-layered samples. The G-line phonon lifetime in the top layer grown from pure EtOH is notably increased and a relative atomic N concentration of $\sim$1/4 allows to conclude that there are comparable fractions of continuous and discontinued SWNTs across the interface of diameter controlled layers of VA-SWNTs.

Acknowledgements

Part of this work was financially supported by the Thailand Research Fund (TRF5780165) and Maejo University; JSPS KAKENHI Grant Numbers JP25107002, JP15H05760, and IRENA Project by JST-EC DG RTD, Strategic International Collaborative Research Program, SICORP. Part of this work is based on results obtained from a project commissioned by the New Energy and Industrial Technology Development Organization (NEDO). We also acknowledge supports from Advanced Characterization Nanotechnology Platform of the University of Tokyo, supported by "Nanotechnology Platform" of the Ministry of Education, Culture, Sports, Science and Technology (MEXT), Japan. CK acknowledges the Austrian Academy of Sciences for the APART fellowship A-11456.

References

1 Z. Yao, H. W. C. Postma, L. Balents and C. Dekker, *Nature*, 1999, **402**, 273–276.
2 G. W. Ho, A. T. S. Wee and J. Lin, *Applied Physics Letters*, 2001, **79**, 260–262.
3 S. K. Doorn, M. J. O'Connell, L. Zheng, Y. T. Zhu, S. Huang and J. Liu, *Phys. Rev. Lett.*, 2005, **94**, 016802.
4 Y. Yao, Q. Li, J. Zhang, R. Liu, L. Jiao, Y. T. Zhu and Z. Liu, *Nat. Mater.*, 2007, **6**, 283–286.
5 G. Ning and H. Shinohara, *Chem. Asian J.*, 2009, **4**, 955–960.
6 W. Zhu, A. Rosen and K. Bolton, *J. Chem. Phys.*, 2008, **128**, 124708.
7 T. Thurakitseree, C. Kramberger, A. Kumamoto, S. Chiashi, E. Einarsson and S. Maruyama, *ACS Nano*, 2013, **7**, 2205–2211.
8 R. Xiang, Z. Zhang, K. Ogura, J. Okawa, E. Einarsson, Y. Miyauchi, J. Shiomi and S. Maruyama, *Jpn. J. Appl. Phys.*, 2008, **47**, 1971–1974.
9 Y. Murakami, Y. Miyauchi, S. Chiashi and S. Maruyama, *Chem. Phys. Lett.*, 2003, **377**, 49–54.
10 Z. Zhang, E. Einarsson, Y. Murakami, Y. Miyauchi and S. Maruyama, *Phys. Rev. B*, 2010, **81**, 165442.
11 S. Chiashi, Y. Murakami, Y. Miyauchi and S. Maruyama, *Jpn. J. Appl. Phys.*, 2008, **47**, 2010–2015.
12 P. M. Ajayan, T. W. Ebbesen, T. Ichihashi, S. Iijima, K. Tanigaki and H. Hiura, *Nature*, 1993, **362**, 522–525.
13 S. Gayen, S. N. Behera and S. M. Bose, *Phys. Rev. B*, 2007, **76**, 165433.
14 P. M. Ajayan and S. lijima, *Nature*, 1993, **361**, 333–334.
15 H. C. Choi, S. Y. Bae, W.-S. Jang, J. Park, H. J. Song, H.-J. Shin, H. Jung and J.-P. Ahn, *J. Phys. Chem. B*, 2005, **109**, 1683–1688.
16 P. Ayala, A. Grüneis, T. Gemming, D. Grimm, C. Kramberger, M. H. Rümmeli, F. L. Freire, H. Kuzmany, R. Pfeiffer, A. Barreiro, B. Büchner and T. Pichler, *J. Phys. Chem. C*, 2007, **111**, 2879–2884.
17 E. Ibrahim, V. O. Khavrus, A. Leonhardt, S. Hampel, S. Oswald, M. H. Rümmeli and B. Büchner, *Diamond Relat. Mater.*, 2010, **19**, 1199–1206.
18 C. Kramberger, T. Thurakitseree, H. Koh, Y. Izumi, T. Kinoshita, T. Muro, E. Einarsson and S. Maruyama, *Carbon*, 2013, **55**, 196–201.
19 J. Scofield, *J. Electron Spectrosc. Relat. Phenom.*, 1976, **8**, 129–137.
20 W.-T. Chen, Y. Yamada, G.-N. Liu, A. Kubota, T. Ichikawa, Y. Kojima, G.-C. Guo and S. Fukuzumi, *Dalton Trans.*, 2011, **40**, 12826–12831.
21 C. R. Brundle, *J. Vac. Sci. Technol.*, 1976, **13**, 301–309.
22 O. Björneholm, A. Nilsson, A. Sandell, B. Hernnäs and N. Mrtensson, *Phys. Rev. Lett.*, 1992, **68**, 1892–1895.
23 P. Ayala, Y. Miyata, K. De Blauwe, H. Shiozawa, Y. Feng, K. Yanagi, C. Kramberger, S. R. P. Silva, R. Follath, H. Kataura and T. Pichler, *Phys. Rev. B*, 2009, **80**, 205427.
24 D. B. Geohegan, A. A. Puretzky, J. J. Jackson, C. M. Rouleau, G. Eres and K. L. More, *ACS Nano*, 2011, **5**, 8311–8321.
25 Y. Murakami, E. Einarsson, T. Edamura and S. Maruyama, *Phys. Rev. Lett.*, 2005, **94**, 087402.
26 V. P. Sokhan, D. Nicholson and N. Quirke, *J. Chem. Phys.*, 2004, **120**, 3855–3863.

Graphical Abstract

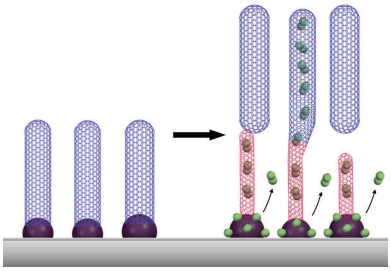

We demonstrate continuous SWNTs throughout double layered arrays with different diameters using encapsulated N_2 molecules as markers to doubtlessly identify seamless interconnections in macroscopic samples.

Electronic Supplementary Information (ESI)

Fingerprinting Seamless Single-Walled Carbon Nanotube Junctions via Migration of Encapsulated N_2 Molecules

From bottom to top, are arrays of vertically aligned SWNT continuous?

Theerapol Thurakitseree,[*a] Christian Kramberger,[b] Pisith Singjai,[c], Shigeo Maruyama[*d,e]

[a]Maejo University, Chiang Mai, Thailand, [b]University of Vienna, Vienna, Austria, [c]Chiang Mai University, Chiang Mai, Thailand, [d]University of Tokyo, Tokyo, Japan, [e]National Institute of Advanced Industrial Science and Technology, Tsukuba, Japan

[*]Corresponding Author: theerapol@mju.ac.th, maruyama@photon.t.u-tokyo.ac.jp

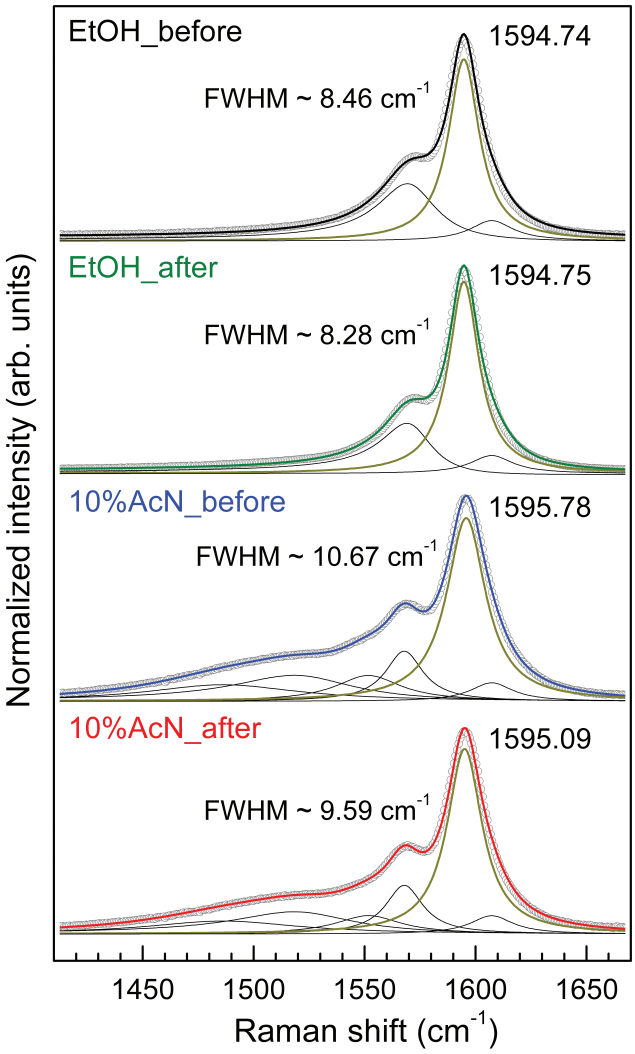

Fig. S1 High frequency G-band spectra of SWNTs before and after removing nanotube cap and annealing. Diminishing in G-band linewidth is due to absence of coulomb interaction from encapsulated N_2 molecules.

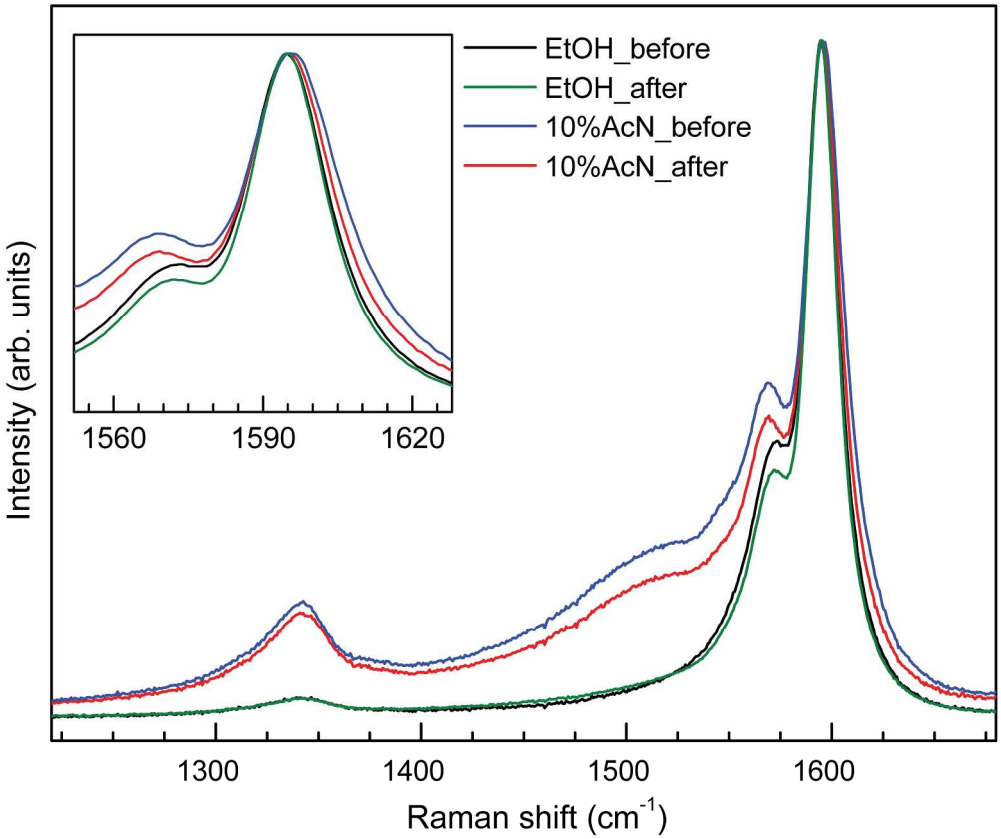

Fig. 1 A comparison of resonance Raman spectra of SWNTs synthesized from ethanol (EtOH) and 10% acetonitrile (10% AcN) before and after annealing at 500°C for 10 min.

247x206mm (300 x 300 DPI)

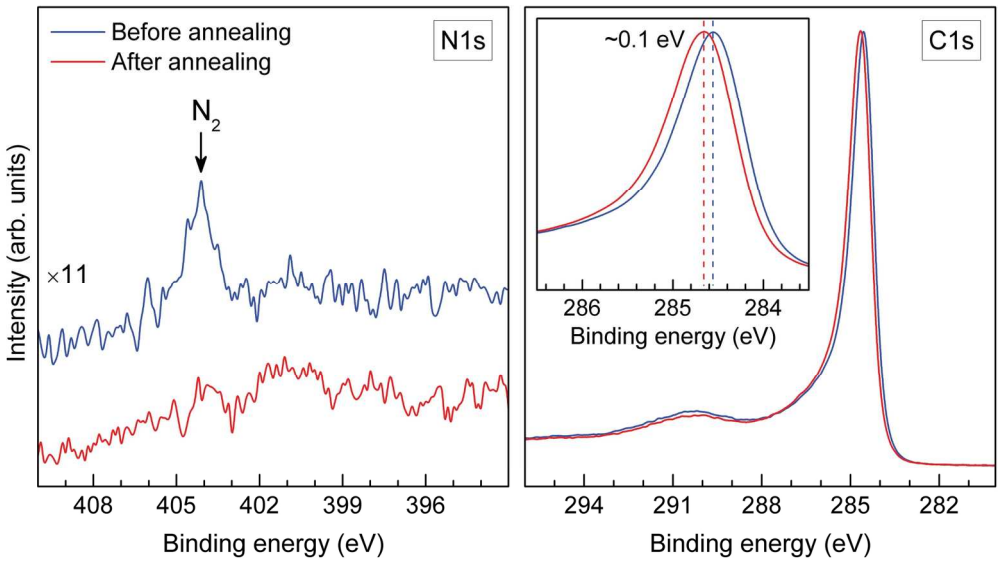

Fig. 2 Photoemission spectra of N-doped SWNT films synthesized from 10% acetonitrile feedstock mixture in ethanol before and after annealing in air at 500°C. The disappearance of N_2 signal was observed after annealing.

164x91mm (300 x 300 DPI)

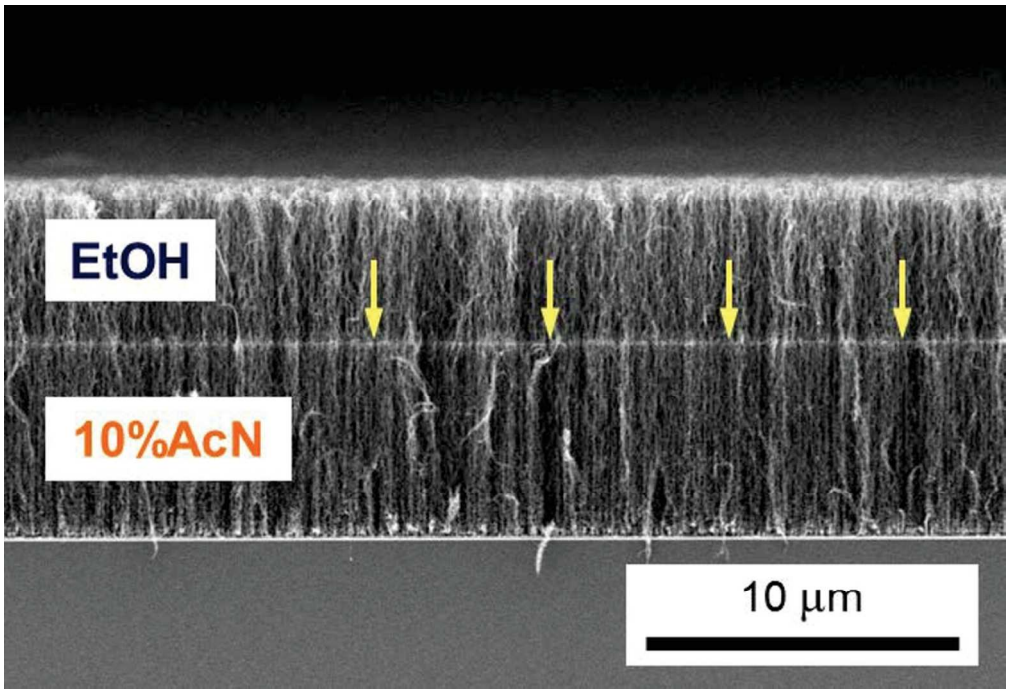

Fig. 3 SEM micrographs of double-layered N-doped SWNT array synthesized from ethanol (EtOH) and 10% acetonitrile feedstock mixture in ethanol (10% AcN), respectively. Yellow arrows highlight the interface between different SWNT arrays at which the feedstock was switched.

77x52mm (300 x 300 DPI)

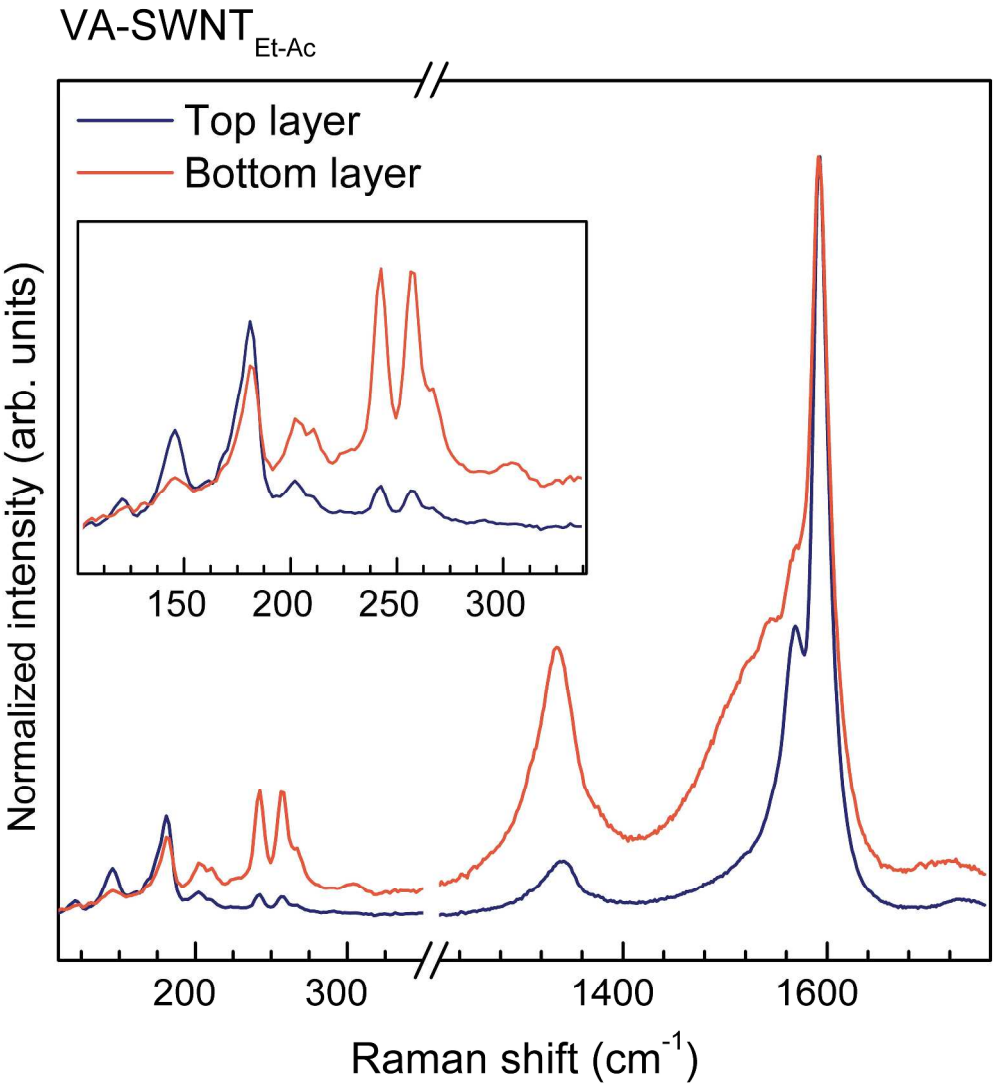

Fig. 4 Cross-sectional resonance Raman spectra of a double-layer VA-SWNT array synthesized from ethanol (top) and
10% acetonitrile (bottom), respectively, indicating root growth mechanism according to feedstock sequence with different nanotube diameters.

322x350mm (300 x 300 DPI)

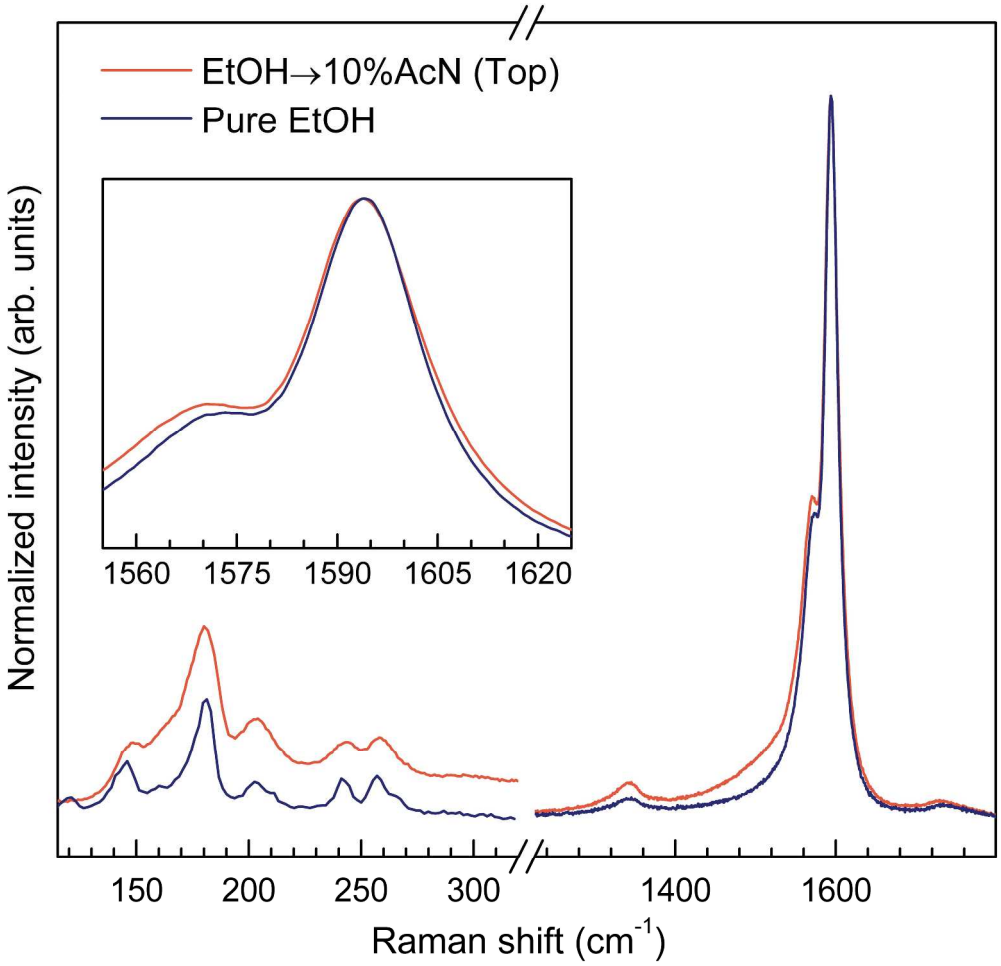

Fig. 5 Raman spectra of a single layered array of $SWNT_{Et}$ from pure EtOH and a layer of $SWNT_{Et}$ with a subsequent layer of $SWNT_{Et\text{-}Ac}$ underneath. The excitation wavelength was 488 nm.

285x274mm (300 x 300 DPI)

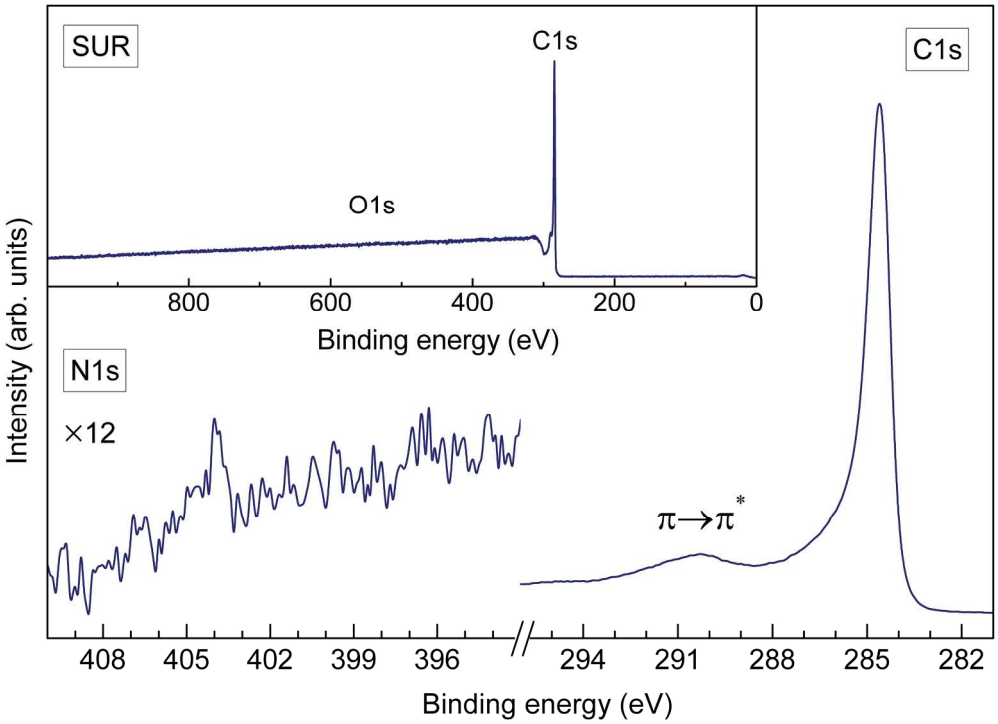

Fig. 6 XPS spectra performed on the top of vertically aligned double-layered SWNT array synthesized from EtOH and 10% AcN, respectively. The molecular N_2 N1s core level is visible. The inset shows the survey scan, indicating very clean sample.

213x153mm (300 x 300 DPI)

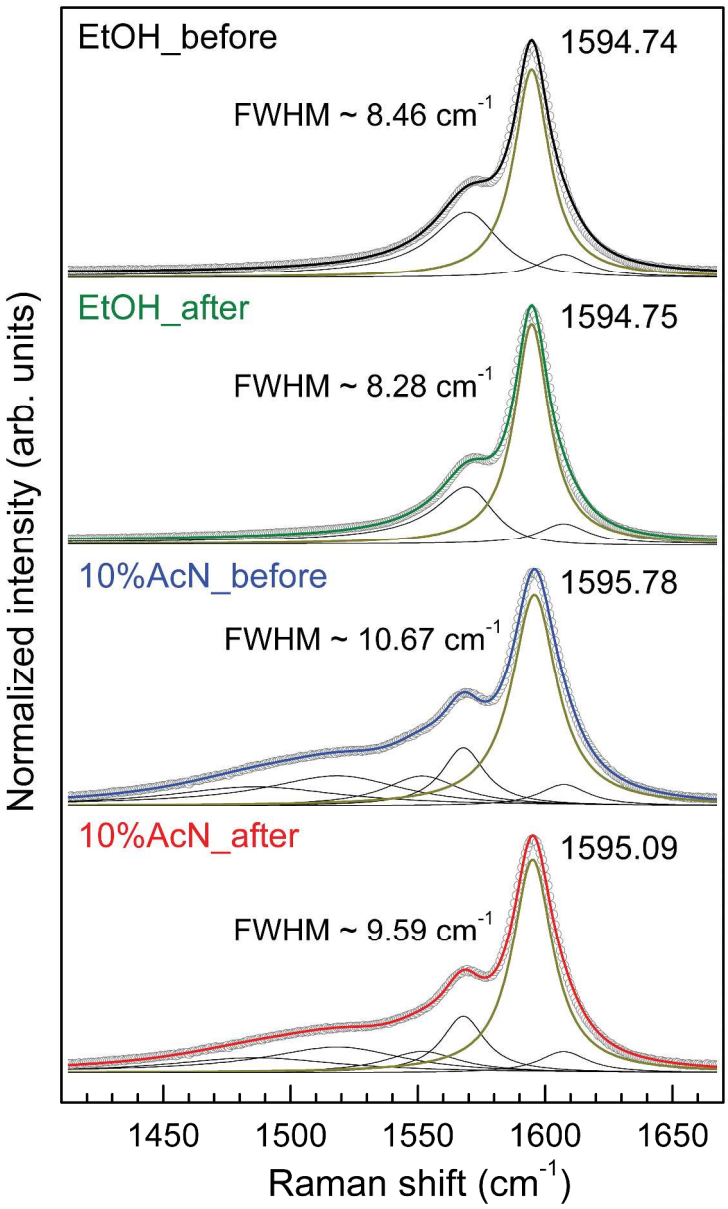

Fig. S1 High frequency G-band spectra of SWNTs before and after removing nanotube cap and annealing. Diminishing in G-band linewidth is due to absence of coulomb interaction from encapsulated N_2 molecules.

489x806mm (300 x 300 DPI)